Investigating the Potential of Ethyl Cellulose and a Porosity- Increasing Agent as a Carrier System for the Formulation of Amorphous Solid Dispersions

Peer-reviewed author version

Everaerts, Melissa; COOLS, Lennert; ADRIAENSENS, Peter; REEKMANS, Gunter; Baatsen, Pieter & Van den Mooter, Guy (2022) Investigating the Potential of Ethyl Cellulose and a Porosity- Increasing Agent as a Carrier System for the Formulation of Amorphous Solid Dispersions. In: Molecular pharmaceutics (Print), 19 (8) , p. 2712 -2724.

DOI: 10.1021/acs.molpharmaceut.1c00972
Handle: http://hdl.handle.net/1942/37978

Investigating the potential of ethyl cellulose and a porosity increasing agent as a carrier system for the formulation of amorphous solid dispersions

Melissa Everaerts[1], Lennert Cools[1], Peter Adriaensens[2], Gunter Reekmans[2], Pieter Baatsen[3] and Guy Van den Mooter[1*].

[1] Drug Delivery and Disposition, KU Leuven, Department of Pharmaceutical and Pharmacological Sciences, Campus Gasthuisberg ON2, Herestraat 49 b921, 3000 Leuven, Belgium.

[2] Applied and Analytical Chemistry, Hasselt University, Institute for Materials Research, Campus Diepenbeek Agoralaan 1-building D, 3590 Diepenbeek, Belgium.

[3] Electron Microscopy Platform & Bio Imaging Core, VIB – KU Leuven Center for Brain & Disease Research, KU Leuven, Department of Neurosciences, Campus Gasthuisberg ON4, Herestraat 49 b602, 3000 Leuven, Belgium.

KEYWORDS: Amorphous solid dispersion; insoluble carrier; ethyl cellulose; porosity increasing agent; ternary solid dispersions

---

ABSTRACT: In the present work an insoluble polymer, i.e. ethyl cellulose (EC), was combined with the water-soluble polyvinylpyrrolidone (PVP) as a carrier system for the formulation of amorphous solid dispersions. The rationale was that by conjoining these two different types of carriers, a more gradual drug release could be created with less risk for precipitation. Our initial hypothesis was that upon contact with the dissolution medium, PVP would be released, creating a porous EC matrix through which the model drug indomethacin could diffuse. Based on observations of EC as a coating material, the effect of the molecular weight of PVP and the ratio of EC/PVP on the miscibility of the polymer blend, the solid-state of the solid dispersion and the drug release from these solid dispersions was investigated. X-ray powder diffraction, modulated differential scanning calorimetry and solid-state nuclear magnetic resonance were used to unravel the miscibility and solid-state properties of these blends and solid dispersions. Solid-state nuclear magnetic resonance appeared to be a crucial technique for this aspect as modulated differential scanning calorimetry was not sufficient to grasp the complex phase behavior of these systems. Both EC/PVP K12 and EC/PVP K25 blends were miscible over the entire composition range and addition of indomethacin did not alter this. Concerning the drug release, it was initially thought that more PVP would lead to a faster drug release with a higher probability that all of the drug molecules would be able to diffuse out of the EC network as more pores would be created. However, this view on the release mechanism appeared to be too simplistic as an optimum was observed for both blends. Based on this work, it could be concluded that drug release

from this complex ternary systems was affected not only by the ratio of EC/PVP and the molecular weight of PVP, but also by interactions between the three components, the wettability of the formulations and the viscosity layer that was created around the particles.

1. INTRODUCTION.

In today's field of drug discovery and development, amorphous solid dispersions (ASDs) are considered to be an effective and successful formulation strategy for poorly water-soluble drugs[1]. A typical ASD formulation comprises an active pharmaceutical ingredient (API) which is molecularly dispersed in an inert carrier and thus lacks the long-range ordering of its crystalline counterpart, leading to a higher apparent solubility[2]. Polymers, especially water-soluble ones, are nowadays considered as the gold standard and are the most commonly used carriers for the formulation of ASDs[3,4]. An important advantage of polymers is their ability to reduce the molecular mobility of the ASD by increasing the glass transition temperature (T_g) and the fact that these carriers can serve as a physical barrier to prevent the nucleation and crystallization of drug molecules[5]. Moreover, polymers can stabilize the ASD in the solid-state through molecular interactions with the API and in the case of water-soluble polymers, also during dissolution of the ASD since the water-soluble polymer can act as a precipitation inhibitor (PI) in aqueous media via similar interactions[6–8]. Despite these advantages, classic binary ASDs based on a water-soluble polymer also feature characteristics which can be potentially detrimental for the stability and the pharmaceutical performance of the ASD. Polyvinylpyrrolidone (PVP) for example, is a well-established polymer for the formulation of ASDs, but also has the characteristic of being highly hygroscopic which in turn can negatively affect the stability of the ASD during processing and storage due to moisture uptake[9,10]. Next to that, most water-soluble polymers will dissolve easily upon contact with the gastrointestinal (GI) fluids, allowing almost immediate liberation of the drug molecules and leading to a rapid increase in drug concentration. A potential pitfall of this swift installation of supersaturation, is the increased risk of precipitation if the water-soluble polymer cannot sufficiently prevent this event. This precipitation subsequently leads to a drop in the concentration profile of the drug and thereby nullifies the solubility advantage of the ASD[11,12].

This phenomenon of precipitation due to rapid drug release is not observed for insoluble carriers where drug release is mediated by a diffusion-controlled process[13]. Ideally, these systems guarantee a more gradual buildup towards supersaturation, associated with less risk for precipitation and thus a prolonged duration of supersaturation as described in our previous work[14]. However, there are also some drawbacks to the use of insoluble polymers as hydrophilic carriers such as poly(2-hydroxyethyl methacrylate) face a limited drug release due to intense physical crosslinking upon contact with water[14]

while more hydrophobic carriers like ethyl cellulose (EC) have a low permeability[15,16]. In addition, water-insoluble carriers cannot function as a PI, meaning that there is no mechanism to protect the drug from precipitation after it has been released from the insoluble matrix.

All the aspects discussed here above make it clear that it can be challenging to find a suitable polymer that answers to all these criteria that are required for a stable ASD with adequate drug release properties. For this reason, a novel generation of ternary ASDs has been introduced where the carrier system consists of a polymer blend instead of a single polymer[9,17,18]. In the present work, the potential of EC in combination with the water-soluble polymer PVP as a carrier system for ASDs was investigated. EC is a popular excipient in the pharmaceutical field with different applications ranging from granulation binder to coatings and sustained-release products[19,20] and is generally regarded as safe[21–23]. Based on what is known from its use as coating material, it was expected that an additional component which increased the porosity of the EC matrix would be required to allow an adequate drug release[24]. Therefore PVP K12 or K25 was incorporated as a porosity increasing agent (PIA) since it was assumed that it would dissolve during the process of drug release, creating free volume to facilitate the diffusion of the drug molecules out of the formulation. Our theory was that due to its hydrophobic properties, the porous EC network that was created during drug release would behave as a rigid matrix and maintain its three-dimensional (3D) shape. Indomethacin (IND), a poorly water-soluble API with a pKa of 4.5 was selected as a model drug to investigate the potential of this carrier system[25].

Since it was expected that the mass transport of the IND molecules would occur predominantly through the porous network that was created, geometry and arrangement of the pores were thought to play a crucial role in the release of the drug molecules from the EC matrix[26]. This was supported by the numerous observations that were already done for EC as a coating material. Various factors such as molecular weight (Mw) of EC, physicochemical properties of the PIA, ratio of EC/PIA, phase behavior, preparation method and process parameters play a critical role in the 3D structure that is created after the PIA has leached out of the coating[26–29]. Our expectation was that these parameters would play a similar role in the EC particles despite the fact that it was not yet known to what extent. Next to that it was, to the best of our knowledge, also not clear what kind of porous network would be ideal for an ASD with delayed yet adequate drug release kinetics. When looking at the application of coatings, a percolation limit has been proposed above which a long-range pathway of interconnected pores is created, allowing efficient diffusion of the molecules from the core to the surface of the coating[26]. In the case of the EC particle which was investigated here, such a structure would translate itself in a continuous porous network as depicted in Figure 1. The opposite phenomenon would be a 3D structure with more discrete pores that are not interconnected.

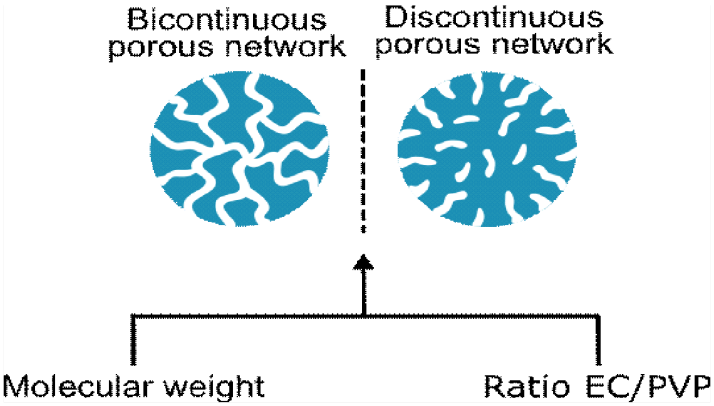

Figure 1 Representation of the possible structures that can be created after the PIA has leached out of the EC matrix. If the pores are interconnected, a continuous porous network is created. In the case of a discontinuous network, the pores are more discrete and closed.

In order to gain more insight on this topic, two aspects that were expected to affect the porous 3D structure and thereby also the drug release kinetics, were selected for further investigation: the effect of Mw of the PIA and the ratio of EC/PIA (Figure 1). One of the goals of this study was to assess the influence of these two parameters on the miscibility of the polymer blend, the solid-state of the ASD and the drug release from these ASDs. With regards to the ratio of EC/PIA, we investigated if a higher amount of PVP in the formulation and hence a higher porosity would lead to faster drug release. This was based on observations from EC coatings with hydroxypropyl cellulose (HPC) as a pore former, where more water-soluble HPC resulted in an increased release rate[28,30,31]. However, since the drug release needed to be adequate in order to guarantee that all of the drug molecules could diffuse out of the formulation, but the release could also not be too fast to minimize the risk for precipitation, it was hypothesized that there would be an optimum in the EC/PVP ratio. In order to investigate all of the forementioned aspects, miscibility of the polymer blends was first studied. After that binary ASDs consisting of IND and EC, PVP K12 or PVP K25 were prepared to assess the drug loadings at which a single amorphous system (based on DSC data) could be obtained. Subsequently, the drug loading was fixed at 30 w% IND for the manufacturing of the ternary ASDs which were subjected to solid-state characterization, determination of the drug loading and drug release testing. The ability of PVP to create a porous EC structure that could maintain its integrity during contact with water was assessed via scanning electron microscopy (SEM).

2. MATERIALS AND METHODS.

2.1. Materials.

IND (PubChem CID: 3715) was purchased from ThermoFisher (Kandel, Germany). EC with a 48.0-49.5% (w/w) ethoxyl content was obtained from Sigma-Aldrich (Zwijndrecht, The Netherlands). PVP K12 and K25 were kindly gifted by BASF (Ludwigshafen, Germany). The chemical structures of IND, EC and PVP are provided in Figure 2.

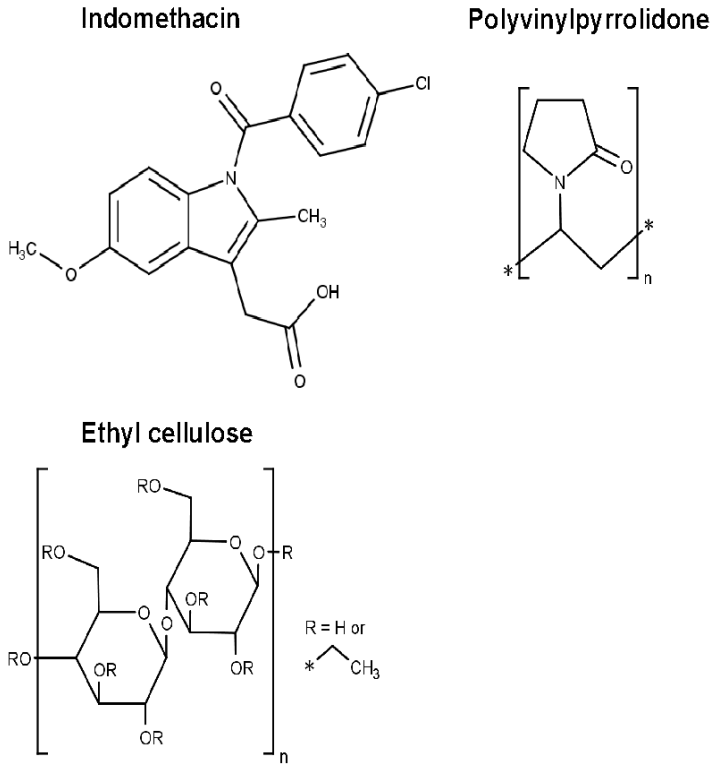

Figure 2 Chemical structures of indomethacin, EC and PVP. Created with MarvinSketch 19.11 (ChemAxon).

Dichloromethane (DCM) and acetonitrile (ACN) were purchased from Fisher Scientific (Loughborough, England). Phosphorus pentoxide and tribasic sodium phosphate dodecahydrate were obtained from ACROS (Geel, Belgium). Sodium phosphate monobasic monohydrate was purchased from Fluka™ (Seelze, Germany) and sodium phosphate dibasic was obtained from Sigma-Aldrich (Steinheim, Germany). 1 M hydrochloric acid was provided by Fisher Scientific (Loughborough, England). Polysorbate 80 and sodium bromide were purchased from Sigma-Aldrich (St. Louis, USA). Purified water was obtained from a Maxima system (Elga Ltd., High Wycombe Bucks, England).

2.2. Preparation of polymer blends and solid dispersions

Polymer blends and solid dispersions were prepared via spray drying or via spraying on a plate at room temperature (RT) to prepare isolated films. In Table 1 an overview is given of the manufacturing techniques, the research objective and the corresponding analysis techniques for the different blends and solid dispersions. Details on the process parameters are provided in section 2.2.1. & 2.2.2.

Table 1 Overview of the purpose, manufacturing and analysis techniques for the different preparations.

	Preparation	Manufacturing technique	Purpose	Analysis techniques
Single polymers	EC	Spray drying & spraying on a plate	Phase behavior of single polymers	mDSC, ssNMR & TGA
	PVP K12	Spray drying		
	PVP K25	Spray drying & spraying on a plate		
Polymer blends	EC/PVP K12	Spray drying	Miscibility and structure after immersion in water	mDSC, ssNMR and SEM
	EC/PVP K25	Spraying on a plate & spray drying		
Solid dispersions	IND/EC	Spray drying	Highest achievable drug loading[1]	XRPD, mDSC, TGA & ssNMR[2]
	IND/PVP K12	Spray drying		
	IND/PVP K25	Spray drying		
	IND/EC/PVP K12	Spray drying	Phase behavior, drug content determination & in vitro drug release	XRPD, mDSC, TGA, release testing & HPLC
	IND/EC/PVP K25	Spray drying		

[1] The highest drug loading at which a fully amorphous system was obtained with no phase separation.

[2] ssNMR measurements were only performed for IND/PVP K12.

2.2.1. Polymer blends

Polymer blends of EC/PVP K12 and EC/PVP K25 were prepared with the following weight percentages of PVP: 0, 5, 10, 20, 50, 80, 90, 95 and 100%. The appropriate amount of EC and PVP was weighed and subsequently dissolved in DCM. The polymer blends of EC/PVP K12 for modulated differential scanning calorimetry (mDSC) and solid-state nuclear magnetic resonance (ssNMR) measurements were prepared via spray drying (Büchi mini spray dryer B-290, Flawil, Switzerland) a 6.67% (w/v) DCM solution. Nitrogen was used as a drying gas at a flow rate of 33 m^3/hour and the inlet temperature was set at 45 °C. The EC/PVP K12 solution was pumped through the nozzle at a feed rate of 10 mL/min and the atomization flow rate was fixed at 10 L/min.

Blends of EC/PVP K25 for mDSC analysis were prepared via a slightly different setup where the polymer solution was sprayed on a glass plate with Teflon coating at RT with an air pressure of 2 bar in

the bifluid nozzle. After one day of drying at RT, the sprayed film was removed from the plate and subsequently grounded to a powder in a mortar using liquid nitrogen. For ssNMR experiments, EC/PVP K25 blends were spray dried (Büchi mini spray dryer B-190, Flawil, Switzerland) applying the same conditions as described for EC/PVP K12 but with air as a drying gas. All EC/PVP K25 solutions that contained less than 80% (w/w) PVP K25 of the total polymer content had a solid content of 6.67% (w/v) while for the higher ratios of PVP K25 a solid content of 3% was used due to the limited solubility of PVP K25 in DCM. After preparation, EC/PVP K12 and EC/PVP K25 blends were dried at RT in a vacuum oven (Mazzali Systems, Monza, Italy) for four consecutive days and stored at –28°C in the presence of phosphorus pentoxide until further analysis.

2.2.2. Solid dispersions

All solid dispersions were spray dried with a Büchi mini spray dryer B-190 (Flawil, Switzerland), set at the same parameters as discussed in section 2.2. with air as drying gas. IND, EC and PVP were dissolved in DCM prior to spray drying. All ASDs discussed here below were subjected to a secondary drying step in the vacuum oven and stored under the same conditions as the polymer blends.

Drug loading of IND in EC was investigated by preparing ASDs containing 10, 20, 30, 40, 50 and 60% (w/w) IND. For PVP K12 and K25 ASDs of 60, 65, 70, 80 and 90% (w/w) IND were spray dried. Solid content of the solutions was 6.67% (w/v) for all ASDs. In addition, amorphous IND was prepared via spray drying a 100 w% IND solution with the same solid content.

For the solid-state analysis and drug release testing, binary and ternary ASDs were spray dried with a drug loading of 30% (w/w) IND and EC/PVP ratios of 100/0, 95/5, 90/10, 80/20, 50/50, 20/80, 10/90, 5/95 and 0/100 (w/w). The solid content was set at 6.67% (w/v) for all ASDs, with the exception of those which contained 80% (w/w) PVP K25 or more of the total polymer content. In that case a solid content of 3% (w/v) was used. For every formulation, three batches were prepared and X-ray powder diffraction (XRPD), mDSC, thermogravimetric analysis (TGA), determination of the drug content and *in vitro* release testing was performed on all batches.

2.3. X-ray powder diffraction (XRPD)

All ASDs were analyzed at RT with an X'pert PRO diffractometer (PANalytical, Almelo, The Netherlands), equipped with a generator set at 45kV and 40mA and a Cu tube (Kα λ=1.5418 Å). Measurements were performed in transmission mode after a small amount of sample was fixated between two Kapton® Polyimide Thin-films (PANalytical, Westborough, USA). The samples were continuously scanned with a 2θ range between 4° to 40°, a step size of 0.0167° and a counting time of 400 s per step. The diffractograms that were obtained, were analyzed with X'Pert Data Viewer Version 1.7 (PANalytical, Almelo, The Netherlands).

2.4. Modulated differential scanning calorimetry (mDSC)

Thermal analysis of the pure compounds, miscibility of the polymer blends and solid state analysis of the ASDs was performed on a Q2000 and Discovery 2500 DSC (TA Instruments, Leatherhead, U.K.), calibrated for temperature, enthalpy and heat capacity with an indium and sapphire standard. For the calibration of the temperature, n-octadecane and tin were also included. Both systems were equipped with a cooling system (RCS90) and dry nitrogen was used as a purge gas at 50 mL/min. Sample preparation was executed by weighing 1-3.5 mg of the compound, blend or ASD in a standard aluminum pan, sealed with the corresponding lid (TA Instruments, Zellik, Belgium). A heat-cool-heat procedure was applied with a heating rate of 2 °C/min, a cooling rat of 20 °C/min, a modulation amplitude of 0.21 °C and a period of 40 s. All samples, with the exception of those containing PVP K25, were heated from -10 °C to 180 °C. In the other case, PVP K25-containing samples were heated to 200 °C. Measurements were always performed in duplicate. Thermograms were analyzed with Trios software version 5.1.1 (TA Instruments, Leatherhead, UK).

2.5. Solid-state nuclear magnetic resonance (ssNMR)

2.5.1. ^{1}H-wideline measurements

^{1}H-wideline ssNMR relaxation measurements were carried out at ambient temperature on a Jeol 600MHz spectrometer in a dedicated Doty Scientific Wide Line probe (DSI-1588) equipped with a 3 mm coil using the solid echo method ($90°_{x'}$ - t_{se} - $90°_{y'}$ - t_{se} - acquire) to overcome the effect of the dead-time of the receiver. The 90° pulse length t_{90} was 2.0 µs and spectra were recorded with a spectral width of 2 MHz (0.5 µs dwell time) allowing an accurate determination of the echo maximum. Samples were placed in 3 mm zirconia rotors which were closed tightly with Kel-F stoppers.

The T_{1H} relaxation decay times (spin-lattice relaxation in the lab frame) were measured by placing an inversion recovery filter in front of the solid echo part ($180°_{x'}$ - t - $90°_{x'}$ - t_{se} - $90°_{y'}$ - t_{se} - acquire). The variable inversion time t was varied between 0.01 and 60 seconds. The integrated proton signal intensity was analyzed mono-exponentially as a function of the variable inversion time t according to the following equation:

$$I(t) = I_0\left[1 - 2\exp exp\left(\frac{-t}{T_{1H}}\right)\right] + c^{te}$$

The $T_{1\rho H}$ relaxation decay times (spin-lattice relaxation in the rotating frame) were measured by applying a spin-lock field (50 kHz) of variable duration, t, after the initial $90°_{x'}$ pulse in the solid echo pulse sequence ($90°_{x'}$ - t - t_{se} -$90°_{y'}$ - t_{se} - acquire). The spin-lock time t was varied between 0.1 and 50 ms. The integrated proton signal intensity was analyzed bi-exponentially as a function of the variable duration of the spin-lock field t_{SL} according to the following equation:

$$I(t) = I_0^{\,S} \exp exp\left(\frac{-t}{T_{1\rho H}^{\,S}}\right) + I_0^{\,L} \exp exp\left(\frac{-t}{T_{1\rho H}^{\,L}}\right) + c^{te}$$

'S' and 'L' refer to the proton fractions with short and long decay time, respectively.

All experimental data were analyzed using a non-linear least-squares fit (Levenberg-Marquardt algorithm). A preparation delay of at least 5 times the longest T_{1H} was always used between successive accumulations to obtain quantitative results.

2.5.2. ^{13}C-cross-polarization/magic angle spinning measurements (^{13}C-CPMAS)

Cross-Polarization (CP) / Magic Angle Spinning (MAS) spectra were acquired on Bruker 400MHz spectrometer (9.4 Tesla) with a 4 mm probe. MAS was performed at 10 kHz. The aromatic signal of hexamethylbenzene was used to calibrate the carbon chemical shift scale (132.1 parts per million, ppm). Acquisition parameters used were: a spectral width of 50 kHz, a 90° pulse length of 4.0 µs, an acquisition time of 20 ms, a recycle delay time of 4 s, a spin-lock field of 50 kHz, a contact time of 1.5 ms and 5000-40000 accumulations. High power proton dipolar decoupling during acquisition was set to 60 kHz.

2.6. Thermogravimetric analysis (TGA)

Residual solvent of the blends and ASDs was determined via weight loss upon heating with a SDT Q600 TGA-analyzer (TA-Instruments, Leatherhead, UK). Samples were heated from RT to 130 °C at a heating rate of 5 °C/min at ambient conditions. In the case of pure EC and PVP K12, an additional measurement was performed in order to monitor thermal degradation of the material by heating the samples to 500 °C and 250 °C respectively. Weight loss and degradation were investigated and calculated with Trios software version 5.1.1 (TA Instruments, Leather-head, UK).

2.7. Scanning electron microscopy (SEM)

For SEM analysis, EC/PVP K12 and EC/PVP K25 blends were spray dried with the following weight percentages of PVP: 10, 50 and 80%. All formulations were prepared with the Büchi mini spray dryer B-190 (Flawil, Switzerland), using the same parameters as discussed in section 2.2. To investigate the porous network that was expected to be created upon contact with water, an aliquot of powder was dispersed in milliQ water. After 2 days, the suspension was centrifuged for 10 min at 20238 x g in a 5424 centrifuge (Eppendorf AG, Hamburg, Germany) and the obtained pellet was dispersed again in fresh milliQ water. These steps were repeated two more times during the next two days. The pellet that was obtained after the last centrifugation step was dried at 40 °C for four consecutive days.

Both the starting material as the suspended and dried powder was analyzed with SEM. For sample preparation, a small amount of powder was deposited on a C-sticker, mounted on an aluminum SEM-pinstub. A coating of 4 or 8 nm Chromium was applied to the powder with the Leica EM ACE600

coater (Vienna, Austria). SEM images were recorded with a Zeiss Sigma scanning electron microscope (Oberkochen, Germany), operated at 5 kV accelerating voltage and a work distance of 7 mm. Secondary electron signals were recorded with an Everhart-Thornley detector biased at 300 V.

2.8. Determination of drug content

Drug content was determined for all ASDs which were subjected to *in vitro* drug release testing by dispersing 20 mg of ASD in 50 mL of ACN. Samples of 3 mL were taken after 1 and 3 days. The withdrawn volume was always replaced with the same volume of ACN. Prior to analysis, samples were filtered through a Chromafil® O-45/15 MS filter with a pore diameter of 0.45 µm (Macherey-Nagel, Düren, Germany). The first 2 mL was used to saturate the filter and discarded. The remaining volume was filtered and analyzed via high-performance liquid chromatography coupled with ultraviolet detection (HPLC-UV) (2.10.) after a 1/1 (v/v) dilution with mobile phase.

2.9. *In vitro* drug release testing

Drug release of the binary and ternary ASDs with a 30% (w/w) drug loading was monitored with a SR8PLUS dissolution paddle apparatus II (Hanson Research, Chatsworth, USA). Paddle rotation speed was set at 100 rpm and the temperature of the dissolution bath at 37 °C. Approximately 166,67 mg of ASD powder, corresponding to 50 mg of IND, was accurately weighed and dispersed in 500 mL HCl medium with 0.5 % (w/v) polysorbate 80 as a wetting agent. The initial pH of the dissolution medium was 1.60. After one hour, the pH was adjusted to 6.80 by the addition of ±35 mL Na_3PO_4 solution (0.25 M) in order to mimic the transition from the stomach to the small intestine. Samples were taken at different time points throughout the experiment, up to five hours after the ASDs had been dispersed in the medium. The withdrawn samples were replaced with the exact same volume of acidic or neutral medium and this replaced volume was included in the calculations of the drug release. The samples were filtered with a Chromafil® O-45/15 MS filter (0.45 µm), purchased from Macherey-Nagel (Düren, Germany). 2mL of sample was always used to saturate the filter with IND and after this, the final mL was injected for HPLC-UV analysis (2.10.) after a 1/1 (v/v) dilution with mobile phase. Drug release was monitored in triplicate for every batch.

2.10. High performance liquid chromatography coupled with ultraviolet detection

Samples for the determination of the drug content and the *in vitro* drug release testing were analyzed with either a Hitachi LaChrom HPLC system (consisting of a L-7100 pump, a L-7420 UV-vis detector, a L-7200 autosampler and a D-7000 interface) or with a Hitachi Chromaster HPLC system (containing a 5160 HPLC pump, a 5410 UV-vis detector and a 5260 autosampler). Data acquisition was performed with the Chromaster System Manager software (version 4.1 and 1.1 respectively). For the analysis, 20 µL of sample was injected in the circuit and pumped through a Nucleodur C18 Gravity 5µm column

(150mm x 4.6 mm) (Macherey-Nagel, Düren, Germany) at a flow rate of 1.0 mL/min and a run time of 6 min. IND was detected at a wavelength of 252 nm. In the case of the Hitachi Chromaster HPLC system, the mobile phase consisted of a phosphate buffer (0.02M) with a pH of 6.80 and ACN (65/35, v/v). For the Hitachi LaChrom HPLC system, another mobile phase was used in addition to the mobile phase which was also used on the Chromaster system: a phosphate buffer (0.02M) with a pH of 6.50 and ACN (60/40, v/v). Both methods were isocratic. Prior to use, all phosphate buffers were filtered through a cellulose acetate filter (0.45 µm), purchased from Sartorius Stedim Biotech GmbH (Göttingen, Germany) and sonicated for at least 30 min. Limit of detection (LOD), limit of quantification (LOQ) and range of linearity for each method can be found in Supplementary information S1.

3. RESULTS AND DISCUSSION.

3.1. Miscibility of the blends

3.1.1. Phase behavior of ethyl cellulose

Prior to investigating the miscibility of EC and PVP, the phase behavior of EC was studied before and after spray drying. In Figure 3, the thermograms of the starting material and the spray dried EC are shown. In the first heating cycle an evaporation peak was detected for the starting product, followed by a glass transition and an endothermic event. The same events were observed for the spray dried EC, but there was an additional exothermic peak (onset at 128 °C) present in this first heating cycle, right after the glass transition. The exothermic event only occurred in the spray dried material and disappeared after the first heating run.

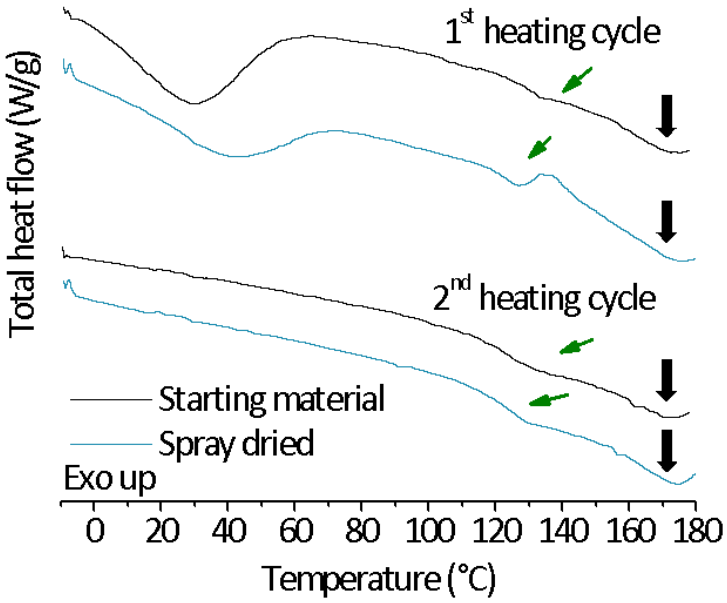

Figure 3 mDSC thermograms of the starting material of EC (black line) and spray dried EC (cyan). Total heat flow of the first and second heating cycle are shown. The black arrow indicates the melting event and the green arrow indicates the T_g. Created with Origin 8.5 from OriginLab (Northampton, USA).

The endothermic event in the thermogram was not due to thermal degradation since mass loss only occurred at temperatures above 190 °C for spray dried EC (Supplementary Information S2). This indicated that the endotherm was due to melting and thus more ordered regions were present before the start of the melting event. In the case of the starting material, these ordered regions were already present at the beginning of the experiment as only a melting peak was observed. However, if EC was dissolved and processed via spray drying, a processing technique which allows fast evaporation of the solvent, a different conformation of EC was obtained with no or less ordered regions as an exothermic peak was detected in the first heating cycle of the spray dried material. During the heating process in the mDSC, the spray dried EC had the tendency to transform back to its more ordered form, which translated itself in an exothermic peak, followed by melting.

In addition to mDSC and TGA experiments, phase behavior of EC was also investigated by looking at the spin lattice relaxation times with ssNMR (Table 2). There was no difference observed for the T_{1H} values, but when looking at a shorter timeframe ($T_{1\rho H}$), subtle differences were noticed for the slow decaying part ($T_{1\rho H}^{L}$). The starting material had a higher $T_{1\rho H}^{L}$ value than the spray dried material, indicating that more ordered regions were present in the initial product. After heating the spray dried EC to 160 °C, the $T_{1\rho H}^{L}$ was again slightly higher and the percentage of the relaxation time had increased. This meant that the heating procedure also had an effect on the material. Nevertheless, caution is needed when interpreting this data as the spin lattice relaxation times are also situated in each other's vicinity.

Table 2 Relaxation times of the starting material, spray dried (SD) EC and SD EC heated to 160 °C. Relaxation times were recorded with a lab (T_{1H}) and rotating ($T_{1\rho H}$) frame. In the case of the rotating frame, a short (^{S}) and long (^{L}) $T_{1\rho H}$ were observed for all three samples. I_0 gives the percentages of both relaxation times.

Sample	T_{1H} (s)	$T_{1\rho H}$ (ms)			
		$T_{1\rho H}^{S}$	I_0^{S} (%)	$T_{1\rho H}^{L}$	I_0^{L} (%)
Starting material	1.0	2.1	11.8	17.8	88.2
SD EC	0.9	2.2	11.9	15.7	88.7
SD heated to 160°C	1.0	2.2	9.6	16.5	90.4

Up until today, there are a limited amount of papers that describe the phase behavior of EC and different phenomena have been reported[32–36]. Davidovich-Pinhas et al.[36] used wide, small and ultra-small angle X-ray scattering to detect a certain degree of order in bulk EC, while Lai et al.[32] even suggested the existence of microcrystals based on hot stage microscopy and quasi-isothermal mDSC. Factors such as Mw, ethoxyl content and the processing technique are of course expected to affect the phase behavior. For this reason, it was important to assess the effect of spray drying on the phase behavior of EC.

3.1.2. Blends of ethyl cellulose and polyvinylpyrrolidone K12

Prior to formulating ternary ASDs, it was important to investigate the miscibility of the polymer blend in the absence of IND. Understanding the miscibility of EC/PVP K12 is a crucial aspect in order to elucidate the phase behavior of the ternary ASDs later on. In addition, incorporation of IND could alter the miscibility behavior and by first studying the blends, this effect could be detected if it occurred. Thermograms of the first heating cycle revealed a single T_g for all weight ratios of EC/PVP K12 (Supplementary Information S3a), meaning that EC/PVP K12 was a miscible system. T_g decreased as there was more PVP K12 in the blend, which was expected as the T_g of pure PVP K12 (107 °C) is lower than the one of pure EC (124 °C). In the thermograms of the blends which contained 50% (w%) PVP K12 or more, a fluctuation of the baseline was observed before the T_g. This was attributed to increased mobility around the T_g region and has already been discussed in the past by Weuts et al.[37] In

the second heating cycle, when the thermal history of the blends was erased, a single T_g remained to be present in all EC/PVP K12 systems (Supplementary Information S3a).

Miscibility of the blends was also confirmed with ssNMR experiments (Table 3). A single 'molar proton fraction averaged' decay time was observed for the blends as their T_{1H} values were situated between those of the pure polymers. With the rotating frame, a bi-exponential trend was detected for all blends, consisting of a short ($T_{1\rho H}^S$) and long ($T_{1\rho H}^L$) relaxation time. For both relaxation times, a similar trend occurred as with the static frame and both relaxation times gradually decreased towards those of pure PVP K12 as more of this compound was incorporated in the blend. Likewise, the percentage of $T_{1\rho H}^S$ increased with more PVP K12, signaling that the protons in the blend gradually started to relax via PVP K12.

Table 3 Spin lattice relaxation times of spray dried EC/PVP K12 blends, recorded with a lab (T_{1H}) and rotating frame ($T_{1\rho H}$). With the rotating frame, a short (^{S}) and a long (^{L}) $T_{1\rho H}$ were observed for the pure compounds and the blends. I_0 gives the percentages of both relaxation times.

EC/PVP K12 (w/w)	T_{1H} (s)	$T_{1\rho H}$ (ms)			
		$T_{1\rho H}^S$	I_0^S (%)	$T_{1\rho H}^L$	I_0^L (%)
100/0	1.0	2.2	12.9	15.4	87.1
95/5	1.0	2.2	13.6	15.2	86.4
90/10	1.1	1.8	13.8	14.6	86.2
80/20	1.1	1.6	15.3	13.6	84.7
50/50	1.3	1.0	17.0	12.0	83.0
20/80	1.6	0.6	20.7	9.6	79.3
10/90	1.9	0.5	22.1	8.6	77.9
5/95	2.0	0.6	21.6	8.5	78.4
0/100	2.1	0.5	24.0	7.8	76.0

3.1.3. Blends of ethyl cellulose and polyvinylpyrrolidone K25

Elucidating the miscibility of the EC/PVP K25 blends appeared to be more challenging compared to that of the EC/PVP K12 blends. The mDSC thermograms of 5 to 50 w% PVP K25 appeared to have two T_gs in the first (Figure 4) and second heating cycle (Supplementary Information S3b). Immiscibility of EC and PVP K25 was previously confirmed by Dereymaker et al.[38] for 25, 50 and 75 w% PVP K25 prepared via spray drying. However, caution is needed with this comparison, as not only the parameters of the manufacturing method were different, but also a different solvent was used. Dereymaker et al. prepared blends via spray drying an ethanolic solution at an inlet temperature of 50 °C. In addition, the second T_g which can be observed here, coincided with the endothermic melting event of EC around 155 °C. It could therefore be wrongly interpreted as a second T_g.

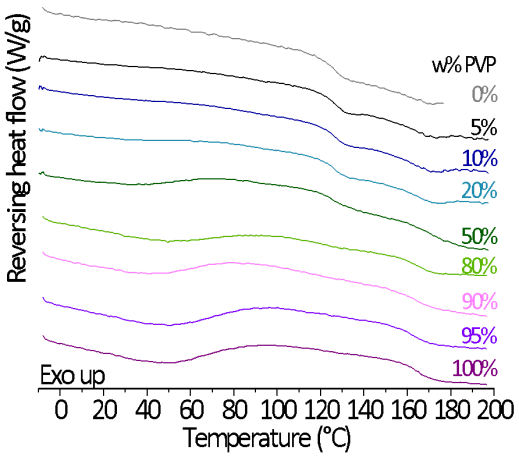

Figure 4 First heating cycle of EC/PVP K25 blends displaying the reversing heat flow. Blends were prepared via spraying on a plate. Created with Origin 8.5 from OriginLab (Northampton, USA).

In order to unambiguously unravel the miscibility behavior of EC/PVP K25, spray dried formulations with 20, 50 and 80 w% PVP K25 were studied via ssNMR to identify the spin lattice relaxation times of the blends (Table 4). The T_{1H} and $T_{1\rho H}$ values of the three compositions are situated between those of pure EC and PVP K25. The T_{1H} values increase as more PVP K25 is present in the blend, while the opposite phenomenon is observed for the $T_{1\rho H}$ values. Based on these results, it could be concluded that EC/PVP K25 was fully miscible. This finding highlights the importance of ssNMR as an essential technique to study the miscibility behavior of this type of complex formulations. If mDSC would have been used here as a stand-alone analysis tool, wrong conclusions could have been made concerning the miscibility behavior of EC/PVP K25.

Table 4 Spin lattice relaxation times of spray dried EC/PVP K25 blends, recorded with a lab (T_{1H}) and rotating frame ($T_{1\rho H}$). With the rotating frame, a short (^{S}) and a long (^{L}) $T_{1\rho H}$ were observed for the pure compounds and the blends. I_0 gives the percentages of both relaxation times.

EC/PVP K25 (w/w)	T_{1H} (s)	$T_{1\rho H}$ (ms)			
		$T_{1\rho H}^S$	I_0^S (%)	$T_{1\rho H}^L$	I_0^L (%)
100/0	1.0	2.2	12.9	15.4	87.1
80/20	1.0	1.3	11.3	15.0	88.7
50/50	1.3	1.1	18.0	13.2	82.0
20/80	1.5	0.6	19.9	11.9	80.1
0/100	1.8	0.5	24.2	10.6	75.8

3.2. Solid state characterization of binary and ternary ASDs

3.2.1. Binary ASDs

3.2.1.1. Indomethacin/ethyl cellulose

To assess the highest drug loading of IND in EC at which a single phase amorphous system was still obtained, binary ASDs with 10, 20, 30, 40, 50 and 60 w% IND were prepared and investigated with XRPD and mDSC. All formulations did not display any Bragg peaks, meaning that they were X-ray amorphous. However, for the drug loading of 60 w% IND, a small endotherm with an onset temperature (T_m) of 153 °C was observed in the total heat flow of the mDSC thermogram, revealing the presence of crystalline material (Supplementary Information S4a). Since no Bragg peaks were detected, it was impossible to conclude if the crystalline material was present as the alpha form (T_m = 154.1 °C)[39] or as the gamma form (T_m = 159.3 °C) of IND displaying melting point depression[14].

3.2.1.2. Indomethacin/polyvinylpyrrolidone K12

XRPD-wise, all IND/PVP K12 formulations were amorphous since no Bragg peaks were detected. According to mDSC, binary IND/PVP K12 ASDs appeared to be amorphous, even at exceptionally high drug loadings (Supplementary Information S4b). For the ASD which contained 90 w% IND, an exothermic event and two melting endotherms were detected during the mDSC experiment.

More information about IND/PVP K12 ASDs was obtained with ssNMR experiments (Table 5). For the formulation with a 30 w% drug loading, $T_{1\rho H}$ values between those of amorphous IND and PVP K12 were obtained and the percentages of the fast and short decaying part were identical to those of amorphous IND. By increasing the drug loading to 60 w% IND, an increase in the $T_{1\rho H}$ values can now be observed. Despite the fact that these values were still situated between those of PVP K12 and amorphous IND, the I_0 values already deviated from amorphous IND, suggesting the possibility of phase separation. When the drug loading was further increased to 80 w%, $T_{1\rho H}^{L}$ corresponded with that of crystalline IND and thus confirmed the presence of crystalline material. It is important to note that if we had only relied on PXRD and mDSC results, an overestimation of the highest possible drug loading would have occurred. The knowledge of the spin lattice relaxation times appeared to be crucial to understand the effect of the drug loading in IND/PVP K12 systems.

Table 5 Spin lattice relaxation times of crystalline IND, amorphous IND, spray dried PVP K12 and IND/PVP K12 ASDs. Lab frame (T_{1H}) recorded two relaxation times for crystalline and amorphous IND. With the rotating frame ($T_{1\rho H}$) a short and long $T_{1\rho H}$ were observed for all samples. I_0 gives the percentages of both relaxation times.

IND/PVP K12 (w/w)	T_{1H} (s)	$T_{1\rho H}$ (ms)			
		$T_{1\rho H}^{S}$	I_0^{S} (%)	$T_{1\rho H}^{L}$	I_0^{L} (%)
Crystalline IND[a]	1.0& 5.1	3.9	20.8	17.0	79.2
Amorphous IND[b*]	1.1& 2.9	2.2	16.8	13.9	83.2
PVP K12	2.1	0.5	24.0	7.8	76.0
30/70	2.1	0.8	16.7	9.4	83.3
60/40	2.1	1.2	10.4	13.2	89.6

80/20	2.1	1.8	10.6	17.4	89.4

[a] I_0 values: 1.0 s (24.8%) & 5.1 s (75.2%)

[b] I_0 values: 1.1 s (37.6%) & 2.9 s (62.4%)

[*] mDSC was used to estimate the amount of residual crystallinity that was present in the sample (8.5 w%).

3.2.1.3. Indomethacin/polyvinylpyrrolidone K25

IND/PVP K25 ASDs were also investigated with XRPD and mDSC. Again, no Bragg peaks were detected for all formulations. mDSC results revealed a small endothermic event around 140 °C for 80 w% IND, but it was so small that it was unclear whether it was caused due to noise or due to melting (Supplementary Information S4c). Based on this mDSC data, it was concluded that IND/PVP K25 was fully amorphous at a drug loading of 70 w% IND or lower.

3.2.2. Ternary ASDs

Incorporation of IND in the polymer blends did not seem to affect their miscibility behavior as the ternary ASDs of both PVP K12 (Figure 5) and K25 (Figure 6) showed a single T_g. Next to that, no crystallinity was detected via mDSC or XRPD. For each formulation three batches were prepared, but the thermograms in Figure 5 and Figure 6 only show one of the three batches. Nevertheless, the thermograms of all batches were recorded and analyzed (Supplementary Information S5, example of IND/EC/PVP K12 - 30/66.5/3.5). The differences in T_g between these batches were within the same range as the differences between two mDSC measurements of the same batch, meaning that similar T_g values were found for the different batches. Regarding the IND/EC/PVP K12 ASDs, an interesting trend was observed concerning the amount of PVP K12 in the ASDs and the T_g. Remember that for the EC/PVP K12 blends a decrease in the T_g was detected as more PVP K12 was added to the blend. Here, it appeared that when the amount of PVP K12 is increased from 0 to 80 w%, the T_g of the ASDs increased as well. This trend can be explained by the formation of hydrogen bonds between IND and PVP K12 via the amide group of PVP and the carboxylic acid group of IND as discussed already by Yuan et al.[40] The T_g values kept increasing until the total polymer content consisted of 80 w% PVP K12. From thereon, the T_g appeared to remain constant, irrespective of the increasing PVP K12 content. This is most likely due to the fact that at a certain threshold, IND is fully involved in hydrogen bonding with PVP K12 and consequently no further increase in T_g is detected.

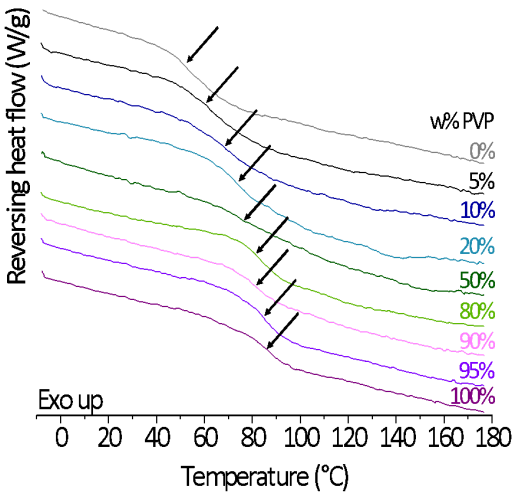

Figure 5 First heating cycle of IND/EC/PVP K12 ASDs displaying the reversing heat flow. Inflections points of the T_gs are indicated with arrows. W% represents the weight fraction of PVP K12 over the total polymer content. Created with Origin 8.5 from OriginLab (Northampton, USA).

IND/EC/PVP K25 ASDs also displayed a single T_g which increased as more PVP K25 was added to the formulation (Figure 6). This could be attributed to the high T_g of PVP K25 (160 °C) and the possible formation of hydrogen bonds between drug and polymer. Likewise as for IND/EC/PVP K12 ASDs, the T_g values appear to remain constant between 80 and 95 w% PVP K25.

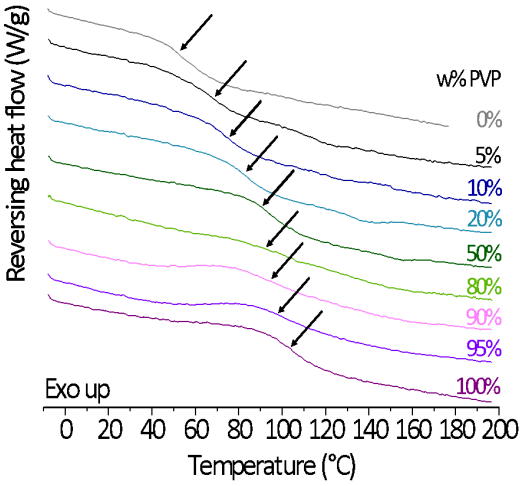

Figure 6 First heating cycle of IND/EC/PVP K25 ASDs displaying the reversing heat flow. Inflections points of the T_gs are indicated with arrows. W% represents the weight fraction of PVP K25 over the total polymer content. Created with Origin 8.5 from OriginLab (Northampton, USA).

3.3. Scanning electron microscopy of the spray dried blends before and after immersion in water

As the formation of pores in the EC matrix was considered to be a crucial part in guaranteeing an adequate drug release, it was important to verify if this porous network was indeed created and maintained during immersion in an aqueous environment. In order to investigate this, SEM images

were recorded of spray dried particles before and after immersion in water (Figure 7). It has to be pointed out that it was not possible to investigate the same particles for the effect of immersion as a Chromium coating needed to be applied for SEM analysis, in order to prevent charging of these non-conductive samples. Nevertheless, a single batch was always used for each composition. Spray dried EC which contained 0 or 10 w% PVP K12 featured both spherical and collapsed particles. When the w% of PVP K12 was further increased to 50 and 80%, collapsed particles were observed with a coarse surface.

Immersion in water did not seem to alter the structure of the particles with 0 or 10 w% PVP K12. In the case of 50 and 80 w% PVP K12 particles, a porous network was observed on the surface after contact with water. These pores were not apparent before the immersion in water. The fact that this porous network was still present after the samples had been immersed in water for four days, confirmed the ability of the EC particle to maintain its rigid structure after PVP K12 diffused out of the formulation. SEM images of EC/PVP K25 blends can be retrieved in Supplementary Information S6. It has to be pointed out that these observations were done for polymer blends and that the addition of IND in the ternary ASDs is expected to also affect the porous network that is created during immersion in water.

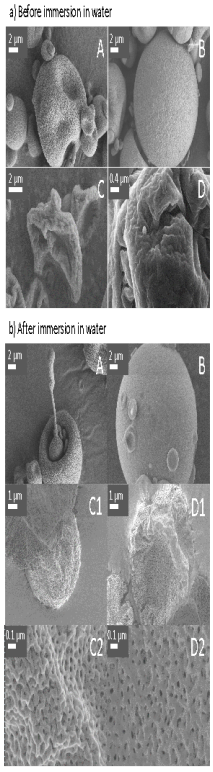

Figure 7 SEM images of spray dried EC/PVP K12 blends before (a) and after (b) immersion in water. The following weight ratios of EC/ PVP K12 were investigated: 100/0 (A), 90/10 (B), 50/50 (C) and 20/80 (D). In case of 50 and 80 w% PVP K12, C2 and D2 give a more detailed image of the porous network that is formed after release of PVP K12.

3.4. *In vitro* drug release

In the introduction, it was hypothesized that more PVP would lead to better and faster drug release, since the carrier system would consist of more water-soluble polymer. However, it was observed that this claim only held to a certain threshold for both PVP K12 and K25 and that an optimum was reached. In Figure 8, release profiles of IND/EC/PVP K12 ASDs are shown. The drug content of these ASDs varied between 27.3 and 31.6 w%, which is close to the theoretical value of 30 w%. Solubilities of crystalline IND in the acidic and neutral medium were experimentally determined in our previous work: 0.7 and 108.3 μg/mL[14]. It has to be noted though that this was in the absence of polysorbate 80 and that the values can therefore be an underestimation since the concentration of polysorbate 80 was above previously reported critical micelle concentration values: 13.4 ± 0.6 mg/L to 24.7 ± 1.4 mg/L[41]. In acidic medium, supersaturation was achieved for all nine formulations as the measured concentrations varied between 12.8 and 46.0 μg/mL. The profile of the binary ASD with PVP K12 reached a plateau in acidic conditions after 45 min while the ternary ASDs appeared to demonstrate a rise in concentration up to 60 min. Once the pH was adjusted to 6.80, all formulations showed a faster drug release after this pH-switch due to the increased solubility of IND. A peculiar trend was observed concerning the ratio of EC/PVP K12 and the drug release. Initially, increasing the amount of PVP K12 from 0 to 20 w% of the total polymer content, led to a faster and better drug release compared to the binary ASD of IND/EC. Increasing the weight fraction of PVP K12 to 50% did not seem to improve the release rate and when the amount of PVP K12 was further raised to 80 w% PVP K12, a dramatic delay in the drug release was noted. This observation coincided with the formation of agglomerates during the *in vitro* drug release testing. This trend was also seen for the calculated areas under the curves (AUC) of the different batches and formulations (see Supplementary Information S7a). Augmenting the weight fraction of PVP K12 to 90 and 95 w% did not result in significantly larger AUCs compared to 80 w% PVP K12. An analysis of variance (ANOVA), followed by a Tukey-Kramer test with both a p-value cutoff of 0.05 revealed that the AUCs of the ternary formulations with 20 and 50 w% PVP K12 of the total polymer content were not statistically different from

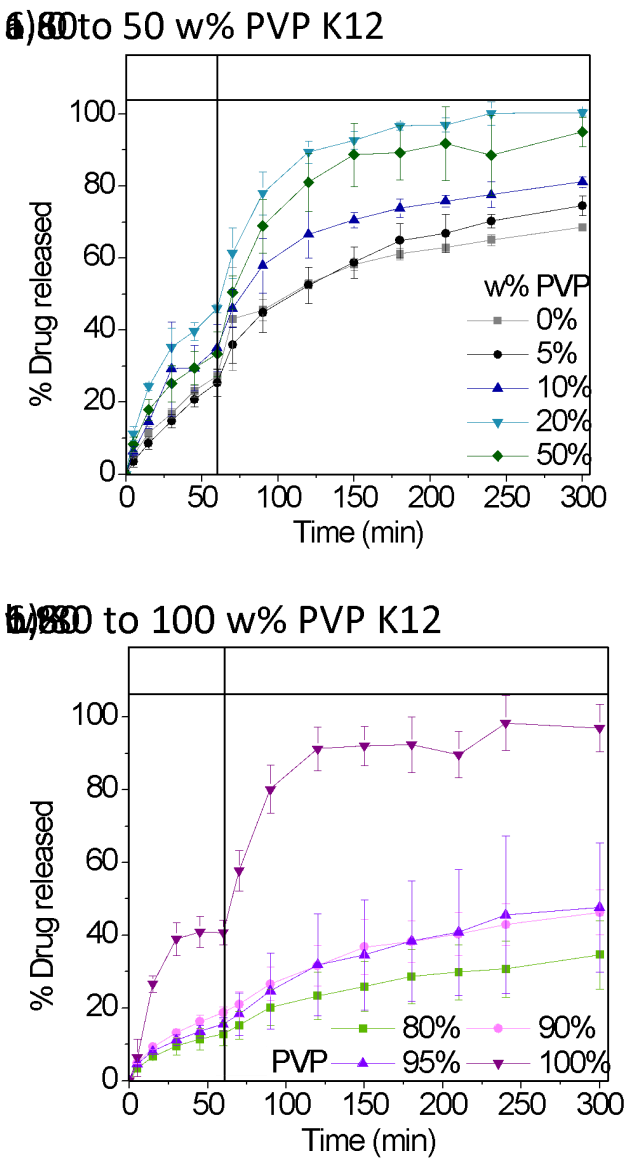

Figure 8 Drug release of IND binary and ternary ASDs with 0 to 50 w% PVP K12 (a) and 80 to 100 w% PVP K12 (b) of the total polymer content. Drug release was monitored in acidic medium (pH 1.60) for 60 min, followed by a pH-switch to neutral conditions (pH 6.80). W% represents the weight fraction of PVP K12 over the total polymer content. Created with Origin 8.5 from OriginLab (Northampton, USA).

The peculiar release performance of IND/EC/PVP K12 ASDs was further investigated. First of all, the behavior of EC/PVP K12 upon immersion in water was studied in absence of IND to identify if the slow drug release for formulations with 80 w% PVP K12 or more could be attributed to a possible interaction between EC and PVP. In Figure 9 pictures are shown of EC/PVP K12 fragments of films prepared via fast solvent evaporation with a Büchi Rotovap R210 (Flawil, Switzerland) at 35 °C (Büchi Heating Bad, Flawil, Switzerland). After addition of water, fragments with 20 and 50 w% PVP K12 remained intact while polymer blends with 80 and 95 w% PVP K12 led to a cloudy appearance of the aqueous medium. This observation hinted towards a possible interaction between EC and PVP upon contact with the dissolution medium at higher w% of PVP K12.

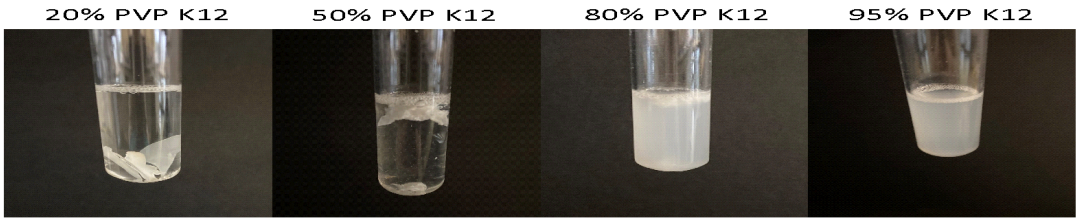

Figure 9 Pictures of EC/PVP K12 fragments immersed in water with 0.5% (m/v) polysorbate 80. W% of PVP K12 are indicated above each picture.

In order to gain more insight into the possible interactions in the ternary ASDs, a ^{13}C cross polarization magic-angle spinning (CPMAS) experiment was performed on the spray dried ternary ASDs (Table 6). The idea was to mimic the aqueous environment during the dissolution by storing the samples at relative humidity (RH) of 57% and compare it with the spectrum of the dry material. Due to the presence of a carbonyl group, a characteristic chemical shift is observed for PVP K12 at 175.4 ppm (Supplementary Information S9). In the ternary ASD, this carbonyl group can form hydrogen bonds with both EC via the hydroxyl groups and IND via the carboxylic acid group. When comparing the different conditions, it is clear that as more PVP K12 is present in the ASD, the difference in chemical shift between the dry and wet sample becomes more pronounced. The formulation with a ratio of 30/3.5/66.5 (w/w/w) IND/EC/PVP K12 for example had a chemical shift at 175.2 ppm before being stored at an elevated humidity, after which the chemical shift had increased to 176 ppm. This indicated that in the dry state, the PVP molecules were less involved in H-bond formation than after exposure to humid conditions. Nonetheless, caution is needed with this interpretation as water is also present in the wet samples and during the dissolution, which can compete for hydrogen bonds[42]. Especially in the case of hydrophilic compounds like PVP, water is expected to outcompete more hydrophobic compounds such as IND and EC. Looking at all of the obtained data, it is obvious that the release mechanism form these ternary ASDs is much more complex as originally thought and described by other authors[30,31,43]. Including more PIA like PVP will lead to more and possibly also larger pores, but will not be the only factor determining the drug release from these systems. It is expected that other aspects like the complex interplay of interactions between the three compounds, the presence of water, the wettability of the ASDs[44], the local viscosity[45] that is created around the spray dried particles and the distribution of the pores will also have an effect on the drug release from these ternary ASDs. Next to that it was observed in our previous work with poly(2-hydroxyethyl methacrylate)[14] that IND molecules in the ASD can crystallize over time during the *in vitro* release experiment. Although this was

not assessed in the present research, it is something that we cannot discard and is also expected to be influenced by the ratio of EC/PVP. Finally, the dissolved fraction of PVP could potentially act as a precipitation inhibitor and thereby positively affect the duration of supersaturation[45].

Table 6 Chemical shift of the carbonyl group of PVP K12 determined via ^{13}C cross polarization magic-angle spinning measurements on dry and wet samples.

IND/EC/PVP K12 (w/w/w)	Dry sample	Wet sample*
EC[a]	/	/
PVP K12	175.4	/[b]
30/35/35	175.6	176.0
30/14/56	175.3	176.0
30/3.5/66.5	175.2	176.0

[a] No shift for EC was detected as it does not contain a carbonyl group.

[b] PVP K12 adsorbed a large quantity of water and it was not feasible to perform ssNMR on this sample after its exposure to the humid conditions.

* A saturated sodium bromide solution was used to generate a RH of 57%.

A similar phenomenon concerning the release was seen for the ternary ASDs of IND/EC/PVP K25 with a drug content between 27.4 and 33.5 w% in Figure 10. When the w% of PVP K25 was increased from 0 to 30 w% of the total polymer content, faster and improved drug release was observed. Again it appeared that there was an optimum concerning the composition since w% of 80 to 95% PVP K25 led to similar AUC values as ASDs with 0 to 10 w% PVP K25 (Supplementary Information S8a). The ternary ASD which consisted of 30 w% PVP K25 of the total polymer content, was the only composition which was not considered to be statistically different from IND/PVP K25 according to the Tukey-Kramer test (Supplementary Information S8b).

Despite the similar trend of having an optimal composition at which all of the drug is able to diffuse out of the formulation, subtle differences were noticed between the two grades of PVP. First of all, for the formulations with less than 50 w% PVP, it appeared that ternary ASDs with PVP K12 performed better than their counterparts with PVP K25. For example, the ternary ASD which consisted of 20 w% PVP K12 resulted in a complete drug release of approximately 100%, while its analogue with PVP K25 had a drug release that fluctuated around 67 to 76% after 5 hours. This first difference in the release profiles can be attributed to the different molecular weights. It is expected that the longer chain length of the PVP K25 molecules will lead to a slower diffusion out of the EC network compared to PVP K12 molecules. In addition, it is anticipated that the PVP molecules which have already diffused out of the formulation, will lead to an increased viscosity in the vicinity of the EC particle. It is therefore not difficult to envision that a larger Mw polymer will also lead to a higher local viscosity. The opposite observation was done for formulations with 80 w% PVP K25 of the total polymer content or higher. The release from these ternary ASDs was indeed also slower and more gradual compared to the formulations with

30 w% PVP K25, but the AUCs were higher than their counterparts with PVP K12 (See Supplementary Information S7a & S8a). This meant that apart from all the factors that have already been discussed above, the Mw of the PIA also played a role in the drug release from these complex ASDs.

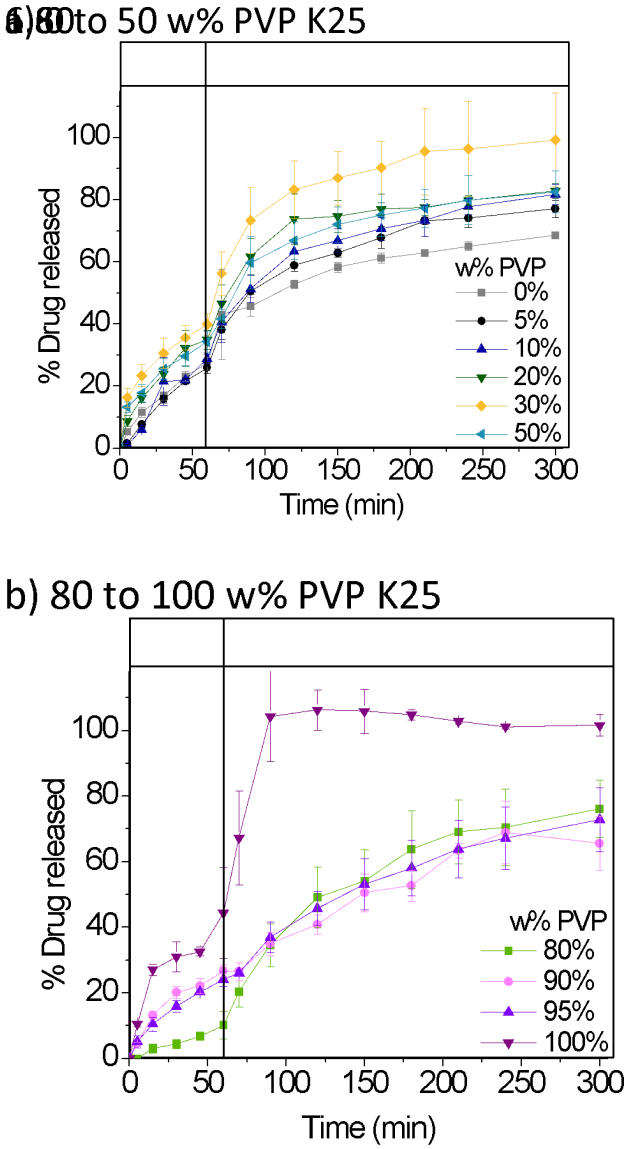

Figure 10 Drug release of IND binary and ternary ASDs with 0 to 50 w% PVP K25 (a) and 80 to 100 w% PVP K25 (b) of the total polymer content. Drug release was monitored in acidic medium (pH 1.60) for 60 min, followed by a pH-switch to neutral conditions (pH 6.80). W% represents the weight fraction of PVP K25 over the total polymer content. Created with Origin 8.5 from OriginLab (Northampton, USA).

4. CONCLUSION.

In this paper the potential of EC as a hydrophobic carrier in combination with PVP as a PIA was investigated for the formulation of ASDs. The carrier system appeared to be promising as the release of IND could be adjusted by changing the ratio of EC/PVP and would thus be an interesting alternative for binary ASDs with only a water-soluble polymer where a limited drug release is observed due to fast supersaturation, followed by precipitation of the drug. In addition the combination that is described here

can also be a viable formulation strategy for ASDs where a controlled release is desired. Considering the solid state analyses, ssNMR appeared to be an essential technique to unravel the miscibility and phase behaviour of the blends and ASDs. If only mDSC and XRPD had been used to study these systems, wrong conclusions and interpretations would have been made. The advantage of using ssNMR to identify the phase behaviour at the nm level and to spatially resolve interactions between the different components has provided invaluable information about these complex ASDs. Moreover, it also gave us more insight into the effect of interactions between the different components during release testing. However given the fact that it was a ternary system with water as a fourth components during the release, made it difficult to fully grasp the different interactions that were taking place. SEM images confirmed our initial hypothesis that pores could be created via the diffusion of PVP and that the hydrophobic nature of EC guaranteed that it could maintain its rigid structure upon contact with water. The release mechanism, which was originally thought to be based on a simple creation of pores, appeared to be considerably more complex. An optimum was detected for both EC/PVP K12 and EC/PVP K25, meaning that the release mechanism was not solely based on incorporating more PIA to create more pores. Factors like interactions, the wettability, the local viscosity, the phase behaviour of the drug during release testing and the Mw are all considered to play a role in the observed release profiles. Overall it is clear that these ternary systems show potential concerning improved release of poorly soluble drugs, but further research is needed in order to completely grasp to what extent the different factors contribute to the release mechanism.

ASSOCIATED CONTENT

Supporting Information. Supplementary information S1: Validation of HPLC methods. Supplementary information S2: Mass loss percentage of spray dried EC. Supplementary information S3: First and second heating cycles of EC/PVP K12 and EC/PVP K25 blends. Supplementary information S4: First heating cycle of binary ASDs. Supplementary information S5: First heating cycle of the three batches of IND/EC/PVP K12 with 5 w% PVP K12 of the total polymer content. Supplementary information S6: SEM images of EC/PVP K25 before and after immersion in water. Supplementary information S7: AUCs and results of Tukey-Kramer test for the release profiles of IND/EC/PVP K12. Supplementary information S8: AUCs and results of Tukey-Kramer test for the release profiles of IND/EC/PVP K25. Supplementary information S9: ^{13}C CPMAS spectra of PVP K12, EC and IND/EC/PVP K12.

This material is available free of charge via the Internet at http://pubs.acs.org.

AUTHOR INFORMATION

Corresponding Author

* e-mail: guy.vandenmooter@kuleuven.be, telephone number: +32 16 330304

Author Contributions

The manuscript was written through contributions of all authors.
All authors have given approval to the final version of the manuscript.

Funding Sources

The authors declare no competing financial interest.

ACKNOWLEDGMENT

We would like to thank Danny Winant from MTM (KU Leuven) for TGA analysis and Gunter Reekmans (Hasselt University) for performing the ssNMR experiments. Next to that, we would like to acknowledge Timothy Pas for his help with the *in vitro* release experiments and Bernard Appeltans for technical support.

ABBREVIATIONS

ACN, acetonitrile; API, active pharmaceutical ingredient; ASDs, amorphous solid dispersions; AUC, area under the curve; CPMAS, cross polarization magic-angle spinning; 3D, three-dimensional; CP, cross-polarization; DCM, dichloromethane; EC, ethyl cellulose; GI, gastrointestinal; HPC, hydroxypropyl cellulose; HPLC-UV, high performance liquid chromatography coupled with ultraviolet detection; IND, indomethacin; LOD, limit of detection; LOQ, limit of quantification; MAS, magic angle spinning; mDSC, modulated differential scanning calorimetry; Mw, molecular weight; PI, precipitation inhibitor; PIA, porosity increasing agent; ppm, parts per million; PVP, polyvinylpyrrolidone; RH, relative humidity; RT, room temperature; SD, spray dried; SEM, scanning electron microscopy; ssNMR, solid-state nuclear magnetic resonance; T_g, glass transition temperature; T_m, melting point onset; TGA, thermogravimetric analysis; XRPD, X-ray powder diffraction.

REFERENCES

(1) Vo, C. L.-N.; Park, C.; Lee, B.-J. Current Trends and Future Perspectives of Solid Dispersions Containing Poorly Water-Soluble Drugs. *European Journal of Pharmaceutics and Biopharmaceutics* **2013**, *85* (3), 799–813. https://doi.org/10.1016/j.ejpb.2013.09.007.

(2) Van den Mooter, G. The Use of Amorphous Solid Dispersions : A Formulation Strategy to Overcome Poor Solubility and Dissolution Rate. *Drug Discovery Today: Technologies* **2012**, *9* (2), e79–e85. https://doi.org/10.1016/j.ddtec.2011.10.002.

(3) Nair, A. R.; Lakshman, Y. D.; Anand, V. S. K.; Sree, K. S. N.; Bhat, K.; Dengale, S. J. Overview of Extensively Employed Polymeric Carriers in Solid Dispersion Technology. *AAPS PharmSciTech* **2020**, *21* (8), 309. https://doi.org/10.1208/s12249-020-01849-z.

(4) Janssens, S.; Van den Mooter, G. Review: Physical Chemistry of Solid Dispersions. *Journal of Pharmacy and Pharmacology* **2009**, *61* (12), 1571–1586. https://doi.org/10.1211/jpp/61.12.0001.

(5) Cid, A. G.; Simonazzi, A.; Palma, S. D.; Bermúdez, J. M. Solid Dispersion Technology as a Strategy to Improve the Bioavailability of Poorly Soluble Drugs. *Therapeutic Delivery* **2019**, *10* (6), 363–382. https://doi.org/10.4155/tde-2019-0007.

(6) Nie, H.; Mo, H.; Zhang, M.; Song, Y.; Fang, K.; Taylor, L. S.; Li, T.; Byrn, S. R. Investigating the Interaction Pattern and Structural Elements of a Drug-Polymer Complex at the Molecular Level. *Molecular Pharmaceutics* **2015**, *12* (7), 2459–2468. https://doi.org/10.1021/acs.molpharmaceut.5b00162.

(7) Chauhan, H.; Kuldipkumar, A.; Barder, T.; Medek, A.; Gu, C. H.; Atef, E. Correlation of Inhibitory Effects of Polymers on Indomethacin Precipitation in Solution and Amorphous Solid Crystallization Based on Molecular Interaction. *Pharmaceutical Research* **2014**, *31* (2), 500–515. https://doi.org/10.1007/s11095-013-1178-1.

(8) Amponsah-Efah, K. K.; Mistry, P.; Eisenhart, R.; Suryanarayanan, R. The Influence of the Strength of Drug–Polymer Interactions on the Dissolution of Amorphous Solid Dispersions. *Molecular Pharmaceutics* **2021**, *18* (1), 174–186. https://doi.org/10.1021/acs.molpharmaceut.0c00790.

(9) Yang, Z.; Nollenberger, K.; Albers, J.; Craig, D.; Qi, S. Microstructure of an Immiscible Polymer Blend and Its Stabilization Effect on Amorphous Solid Dispersions. *Molecular Pharmaceutics* **2013**, *10* (7), 2767–2780.

(10) Rumondor, A. C. F.; Marsac, P. J.; Stanford, L. A.; Taylor, L. S. Phase Behavior of Poly(Vinylpyrrolidone) Containing Amorphous Solid Dispersions in the Presence of Moisture. *Molecular Pharmaceutics* **2009**, *6* (5), 1492–1505. https://doi.org/10.1021/mp900050c.

(11) Sun, D. D.; Lee, P. I. Evolution of Supersaturation of Amorphous Pharmaceuticals: Nonlinear Rate of Supersaturation Generation Regulated by Matrix Diffusion. *Molecular Pharmaceutics* **2015**, *12* (4), 1203–1215. https://doi.org/10.1021/mp500711c.

(12) Sun, D. D.; Lee, P. I. Haste Makes Waste: The Interplay Between Dissolution and Precipitation of Supersaturating Formulations. *The AAPS Journal* **2015**, *17* (6), 1317–1326. https://doi.org/10.1208/s12248-015-9825-6.

(13) Sun, D. D.; Lee, P. I. Probing the Mechanisms of Drug Release from Amorphous Solid Dispersions in Medium-Soluble and Medium-Insoluble Carriers. *Journal of Controlled Release* **2015**, *211*, 85–93. https://doi.org/10.1016/j.jconrel.2015.06.004.

(14) Everaerts, M.; Van den Mooter, G. Complex Amorphous Solid Dispersions Based on Poly(2-Hydroxyethyl Methacrylate): Study of Drug Release from a Hydrophilic Insoluble Polymeric Carrier in the Presence and Absence of a Porosity Increasing Agent. *International Journal of Pharmaceutics* **2019**, *566*, 77–88. https://doi.org/10.1016/j.ijpharm.2019.05.040.

(15) Desai, J.; Alexander, K.; Riga, A. Characterization of Polymeric Dispersions of Dimenhydrinate in Ethyl Cellulose for Controlled Release. *International Journal of Pharmaceutics* **2006**, *308* (1–2), 115–123. https://doi.org/10.1016/j.ijpharm.2005.10.034.

(16) Huang, J.; Wigent, R. J.; Schwartz, J. B. Nifedipine Molecular Dispersion in Microparticles of Ammonio Methacrylate Copolymer and Ethylcellulose Binary Blends for Controlled Drug Delivery: Effect of Matrix Composition. *Drug Development and Industrial Pharmacy* **2006**, *32* (10), 1185–1197. https://doi.org/10.1080/03639040600832827.

(17) Marks, J. A.; Wegiel, L. A.; Taylor, L. S.; Edgar, K. J. Pairwise Polymer Blends for Oral Drug Delivery. *Journal of Pharmaceutical Sciences* **2014**, *103* (9), 2871–2883. https://doi.org/10.1002/jps.23991.

(18) Everaerts, M.; Tigrine, A.; de la Rosa, V. R.; Hoogenboom, R.; Adriaensens, P.; Clasen, C.; Van den Mooter, G. Unravelling the Miscibility of Poly(2-Oxazoline)s: A Novel Polymer Class for the Formulation of Amorphous Solid Dispersions. *Molecules* **2020**, *25* (16), 3587. https://doi.org/10.3390/molecules25163587.

(19) Deshmukh, R. K.; Naik, J. B. Optimization of Spray-Dried Diclofenac Sodium-Loaded Microspheres by Screening Design. *Drying Technology* **2016**, *34* (13), 1593–1603. https://doi.org/10.1080/07373937.2016.1138121.

(20) Wasilewska, K.; Winnicka, K. Ethylcellulose–A Pharmaceutical Excipient with Multidirectional Application in Drug Dosage Forms Development. *Materials* **2019**, *12* (20), 3386. https://doi.org/10.3390/ma12203386.

(21) FDA. GRN No. 470 Ethyl cellulose https://www.cfsanappsexternal.fda.gov/scripts/fdcc/index.cfm?set=GRASNotices&id=470 (accessed 2021 -01 -21).

(22) Joint FAO/WHO Expert Committee on Food Additives. *Evaluation of Certain Food Additives and Contaminants*; 1990.

(23) Younes, M.; Aggett, P.; Aguilar, F.; Crebelli, R.; Di Domenico, A.; Dusemund, B.; Filipič, M.; Frutos, M. J.; Galtier, P.; Gott, D.; Gundert-Remy, U.; Kuhnle, G. G.; Lambré, C.; Leblanc, J.-C.; Lillegaard, I. T.; Moldeus, P.; Mortensen, A.; Oskarsson, A.; Stankovic, I.; Tobback, P.; Waalkens-Berendsen, I.; Wright, M.; Tard, A.; Tasiopoulou, S.; Woutersen, R. A. Re-Evaluation of Celluloses E 460(i), E 460(Ii), E 461, E 462, E 463, E 464, E 465, E 466, E 468 and E 469 as Food Additives. *EFSA Journal* **2018**, *16* (1), 5047. https://doi.org/10.2903/j.efsa.2018.5047.

(24) Ye, Z.; Rombout, P.; Remon, J. P.; Vervaet, C.; Van den Mooter, G. Correlation between the Permeability of Metoprolol Tartrate through Plasticized Isolated Ethylcellulose/Hydroxypropyl Methylcellulose Films and Drug Release from Reservoir Pellets. *European Journal of Pharmaceutics and Biopharmaceutics* **2007**, *67* (2), 485–490. https://doi.org/10.1016/j.ejpb.2007.02.010.

(25) National Center for Biotechnology Information. PubChem Compound Database; CID=3715, Indomethacin https://pubchem.ncbi.nlm.nih.gov/compound/Indomethacin (accessed 2021 -01 -22).

(26) Andersson, H.; Hjärtstam, J.; Stading, M.; von Corswant, C.; Larsson, A. Effects of Molecular Weight on Permeability and Microstructure of Mixed Ethyl-Hydroxypropyl-Cellulose Films. *European Journal of Pharmaceutical Sciences* **2013**, *48* (1–2), 240–248. https://doi.org/10.1016/j.ejps.2012.11.003.

(27) Sakellariou, P.; Rowe, R. C. The Morphology of Blends of Ethylcellulose with Hydroxypropyl Methylcellulose as Used in Film Coating. *International Journal of Pharmaceutics* **1995**, *125* (2), 289–296. https://doi.org/10.1016/0378-5173(95)00147-B.

(28) Marucci, M.; Hjärtstam, J.; Ragnarsson, G.; Iselau, F.; Axelsson, A. Coated Formulations: New Insights into the Release Mechanism and Changes in the Film Properties with a Novel Release Cell. *Journal of Controlled Release* **2009**, *136* (3), 206–212. https://doi.org/10.1016/j.jconrel.2009.02.017.

(29) Sakellariou, P.; Rowe, R. C.; White, E. F. T. A Study of the Leaching/Retention of Water-Soluble Polymers in Blends with Ethylcellulose Using Torsional Braid Analysis. *Journal of Controlled Release* **1988**, *7* (2), 147–157. https://doi.org/10.1016/0168-3659(88)90006-5.

(30) Thombre, A. G.; DeNoto, A. R.; Falkner, F. C.; Lazar, J. D. In Vitro/in Vivo Correlations of Sustained-Release Coated Multiparticulate Formulations of Doxazosin. *International Journal of Pharmaceutics* **1994**, *111* (2), 181–189. https://doi.org/10.1016/0378-5173(94)00137-5.

(31) Umprayn, K.; Chitropas, P.; Amarekajorn, S. Development of Terbutaline Sulfate Sustained-Release Coated Pellets. *Drug Development and Industrial Pharmacy* **1999**, *25* (4), 477–491. https://doi.org/10.1081/DDC-100102198.

(32) Lai, H. L.; Pitt, K.; Craig, D. Q. M. Characterisation of the Thermal Properties of Ethylcellulose Using Differential Scanning and Quasi-Isothermal Calorimetric Approaches. *International Journal of Pharmaceutics* **2010**, *386* (1–2), 178–184. https://doi.org/10.1016/j.ijpharm.2009.11.013.

(33) Jianan, C.; Yifang, H.; Jinyue, Y.; Shaoqiong, Y.; Hua, Y. Thermotropic Liquid Crystalline Behaviors of Ethylcellulose. *Journal of Applied Polymer Science* **1992**, *45* (12), 2153–2158. https://doi.org/10.1002/app.1992.070451211.

(34) Mahnaj, T.; Ahmed, S. U.; Plakogiannis, F. M. Characterization of Ethyl Cellulose Polymer. *Pharmaceutical Development and Technology* **2013**, *18* (5), 982–989. https://doi.org/10.3109/10837450.2011.604781.

(35) Bidault, O.; Assifaoui, A.; Champion, D.; Le Meste, M. Dielectric Spectroscopy Measurements of the Sub-Tg Relaxations in Amorphous Ethyl Cellulose: A Relaxation Magnitude Study. *Journal of Non-Crystalline Solids* **2005**, *351* (14–15), 1167–1178. https://doi.org/10.1016/j.jnoncrysol.2005.03.014.

(36) Davidovich-Pinhas, M.; Barbut, S.; Marangoni, A. G. Physical Structure and Thermal Behavior of Ethylcellulose. *Cellulose* **2014**, *21* (5), 3243–3255. https://doi.org/10.1007/s10570-014-0377-1.

(37) Weuts, I.; Kempen, D.; Six, K.; Peeters, J.; Verreck, G.; Brewster, M.; Van den Mooter, G. Evaluation of Different Calorimetric Methods to Determine the Glass Transition Temperature and Molecular Mobility below Tg for Amorphous Drugs. *International Journal of Pharmaceutics* **2003**, *259* (1–2), 17–25. https://doi.org/10.1016/S0378-5173(03)00233-3.

(38) Dereymaker, A.; Scurr, D. J.; Steer, E. D.; Roberts, C. J.; Van den Mooter, G. Controlling the Release of Indomethacin from Glass Solutions Layered with a Rate Controlling Membrane Using Fluid-Bed Processing. Part 1: Surface and Cross-Sectional Chemical Analysis. *Molecular Pharmaceutics* **2017**, *14* (4), 959–973. https://doi.org/10.1021/acs.molpharmaceut.6b01023.

(39) Surwase, S. A.; Boetker, J. P.; Saville, D.; Boyd, B. J.; Gordon, K. C.; Peltonen, L.; Strachan, C. J. Indomethacin: New Polymorphs of an Old Drug. *Molecular Pharmaceutics* **2013**, *10* (12), 4472–4480. https://doi.org/10.1021/mp400299a.

(40) Yuan, X.; Xiang, T.-X.; Anderson, B. D.; Munson, E. J. Hydrogen Bonding Interactions in Amorphous Indomethacin and Its Amorphous Solid Dispersions with Poly(Vinylpyrrolidone) and Poly(Vinylpyrrolidone-Co-Vinyl Acetate) Studied Using 13C Solid-State NMR. *Molecular Pharmaceutics* **2015**, *12* (12), 4518–4528. https://doi.org/10.1021/acs.molpharmaceut.5b00705.

(41) Braun, A. C.; Ilko, D.; Merget, B.; Gieseler, H.; Germershaus, O.; Holzgrabe, U.; Meinel, L. Predicting Critical Micelle Concentration and Micelle Molecular Weight of Polysorbate 80 Using Compendial Methods. *European Journal of Pharmaceutics and Biopharmaceutics* **2015**, *94*, 559–568. https://doi.org/10.1016/j.ejpb.2014.12.015.

(42) Ueda, K.; Higashi, K.; Yamamoto, K.; Moribe, K. The Effect of HPMCAS Functional Groups on Drug Crystallization from the Supersaturated State and Dissolution Improvement. *International Journal of Pharmaceutics* **2014**, *464* (1–2), 205–213. https://doi.org/10.1016/j.ijpharm.2014.01.005.

(43) Boel, E.; Smeets, A.; Vergaelen, M.; De la Rosa, V. R.; Hoogenboom, R.; Van den Mooter, G. Comparative Study of the Potential of Poly (2-Ethyl-2-Oxazoline) as Carrier in the Formulation of Amorphous Solid Dispersions of Poorly Soluble Drugs. *European Journal of Pharmaceutics and Biopharmaceutics* **2019**, *144*, 79–90. https://doi.org/10.1016/j.ejpb.2019.09.005.

(44) Lu, Y.; Tang, N.; Lian, R.; Qi, J.; Wu, W. Understanding the Relationship between Wettability and Dissolution of Solid Dispersion. *International Journal of Pharmaceutics* **2014**, *465* (1–2), 25–31. https://doi.org/10.1016/j.ijpharm.2014.02.004.

(45) Wang, W.; Li, M.; Yang, Q.; Liu, Q.; Ye, M.; Yang, G. The Opposed Effects of Polyvinylpyrrolidone K30 on Dissolution and Precipitation for Indomethacin Supersaturating Drug Delivery Systems. *AAPS PharmSciTech* **2020**, *21* (3), 107. https://doi.org/10.1208/s12249-020-01647-7.

TOC